

Chapter 1

INTRODUCTION

1.1 Opening Remarks

The Madden-Julian oscillation (MJO) is a tropical weather phenomenon in which wave disturbances form quasi-periodically in the Indian ocean and propagate eastward. These disturbances exist on an intraseasonal time scale [longer than synoptic time scales (~ 2 weeks), though shorter than a season (90 days) (Lau and Waliser, 2005)] and consist of a convective region and its surrounding flow field. This wave pulse travels along the equator at an average speed of 5 ms^{-1} until it reaches the central Pacific where the convection dissipates due to lower sea surface temperatures. This marks the transition of the MJO from the convective phase to the dry phase, where the forced waves are free to propagate away. The dry phase is essentially the continued eastward movement of the now decoupled Kelvin response which travels at its free wave speed. This study is restricted to the convective phase of the MJO lifecycle.

By filtering outgoing longwave radiation (OLR) time series data for frequencies and wavenumbers characteristic of the MJO, a composite lifecycle of MJO convection can be constructed. In this view the negative OLR anomalies are used as a proxy for the convective region. Fig. 1.1 consists of panels at 6 day intervals showing the evolution of the OLR anomaly associated with the MJO during its convective phase.

The next section will discuss some of the literature regarding the MJO. As a testament to its complexity, the material available on this subject is vast and covers many facets. Since an exhaustive survey is not appropriate here, the following treatment will attempt

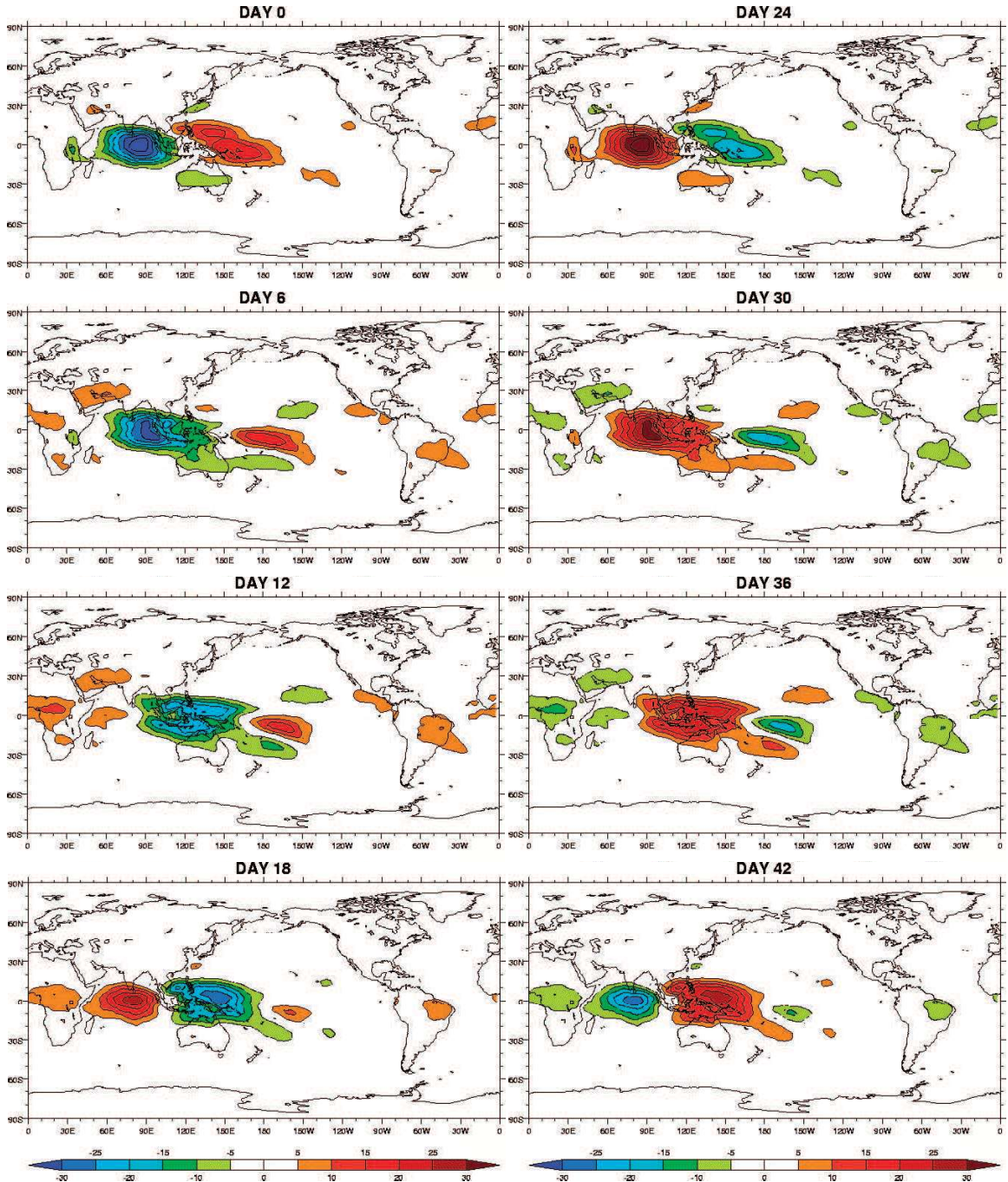


Figure 1.1: A composite lifecycle of MJO convection as seen through filtered OLR time series data. Negative OLR anomalies (cool colors) are used as a proxy for enhanced convection, denoting an active phase of the oscillation. Positive OLR anomalies (warm colors) are used as a proxy for suppressed convection, corresponding to an inactive phase. This figure is composed of select time snap shots originally from an animation (Matthews).

to establish the basic characteristics of the MJO (especially those most relevant to this study), as well as briefly cover modeling efforts and theoretical work. It's acknowledged that some well documented aspects, deemed not as crucial to this study, have been left out. In addition, only a sampling of the influential papers on the topics addressed were able to be covered. To mitigate this, some comprehensive reviews are mentioned which provide an introduction to many interesting aspects of this phenomenon and also contain references for further study.

1.2 Literature Review

The phenomenon most commonly referred to as the Madden-Julian oscillation (MJO) was discovered in 1970 by Roland Madden and Paul Julian (hereafter referred to as MJ) during research stimulated by the discovery of the Quasibiennial oscillation (QBO) (Madden and Julian, 2005). By spectrally analyzing approximately 10 years of rawinsonde data from Canton Island (3°S , 172°W) over a broad range of frequencies they observed an oscillation in the station pressure and zonal wind with a frequency lower than that of any hypothesized wave mode, but higher than any seasonal variation. Based on its spectral peak in the frequency range associated with periods of 41–53 days, MJ referred to the finding as a 40–50 day oscillation. They also reported that the low-level and upper-level zonal wind and pressure fields were out of phase and concluded the new phenomenon could most adequately be described as a large circulation cell oriented in the equatorial zonal plane (Madden and Julian, 1971). A year later MJ published a follow-up paper involving cross-spectral analysis of time series data from stations located in the tropics to study the spatial scale of the 40–50 day oscillation (Madden and Julian, 1972). Their results suggested that the oscillation has a global scale zonally but is restricted to the tropics (10°S , 10°N), and possessed features of a wave moving eastward from the Indian ocean to the eastern Pacific whose characteristics changed with time. The paper concluded by summarizing what was known about the oscillation at the time in a schematic (see Fig. 1.2).

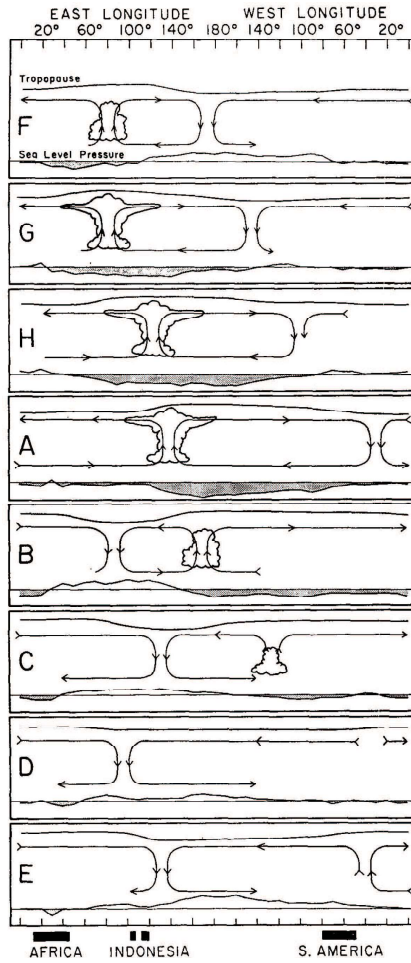


Figure 1.2: Reproduced from Madden and Julian (1972). Depicts the time and space variations in the zonal plane associated with the 40–50 day oscillation. Mean sea level pressure anomalies are represented in the bottom of each panel by the curve that deviates from the straight line, where the negative anomalies are shaded. The sketched cumulus clouds represent regions of enhanced large-scale convection, with streamlines indicating the associated zonal circulation. The curve at the top of each panel represents the relative tropopause height. Block continents are found at the bottom of the figure, and relative dates are given by letters (indexed from the surface low pressure anomaly at Canton Island). **F** - Surface low pressure anomaly over East Africa and the Indian ocean. Large scale convection initiates over the Indian ocean. Circulation cells form. **G** - Convection strengthens, pressure anomaly and eastern circulation cell spread eastward. **H** - Convection moving east across Indonesia. **A** - Surface low pressure anomaly over Canton Island. **B** - Convection starts to weaken, western circulation cell shrinks, and descending branch of circulation characteristic of the inactive phase is seen to the west. **C** - Convection decays further in the colder waters of the central Pacific. **D** - Convection is dead, subsidence dominates Indonesia. **E** - Subsiding branch continues to move east, surface high pressure anomaly over Canton Island, dry phase signal seen on eastern side of South America.

Space-time spectral analysis on 8-years of outgoing longwave radiation (OLR) data was employed by Nakazawa (1986) to look at the mean features of intraseasonal variation (ISV), in which he found strong power between the periods of 30–60 days. In this time range he identified clustering of active convective regions consisting of multiple synoptic scale convective cells with horizontal scale $O(1000 \text{ km})$ and a lifecycle of less than 10 days. He noted that both the 30–60 day variation and the synoptic scale convective regions it contained moved eastward. Nakazawa (1988) gave further detail of the fine structure within the convective region by analyzing 3-hourly geostationary satellite infrared data. The outcome was a heirarchial view of the convective components contained in an ISV envelope. The synoptic scale cells mentioned above were given the name “super clusters” (a term which is avoided during discussion of our convective forcing due to ambiguity), and were seen to be composed of mesoscale “cloud clusters” (CC), having a horizontal scale of $O(100 \text{ km})$. Surprisingly, these CC which have a lifecycle of 1–2 days, travel westward. It is by the successive eastward formation of each westward traveling CC that the super cluster moves eastward. These features are seen explicitly in the Hovmoller diagrams of Fig. 1.3.

Another look at the convective organization, and in addition the accompanying large-scale circulation disturbances, is provided by Hendon and Liebmann (1994). Composite lifecycles are constructed by regression of band-pass filtered winds, divergences, MSUT (microwave sounding unit temperature), and OLR for MJO episodes within an 11-year record that have a discrete large-scale convective signal present. The motivating question is whether the oscillation simply organizes existing convection on all scales such that co-operative growth with the circulation occurs, or if the multi-scale convective structure is responsible for the evolution of the oscillation. They observed that synoptic-scale variability is strongly modulated within the convective envelope, and that feedback between the circulation and convection occurs at this scale, though no predominant mode was detected. On the mesoscale, a predominant mode of variability with ~ 2 -day period was observed, though its small variance suggested its role in the MJO was more one of effect rather than

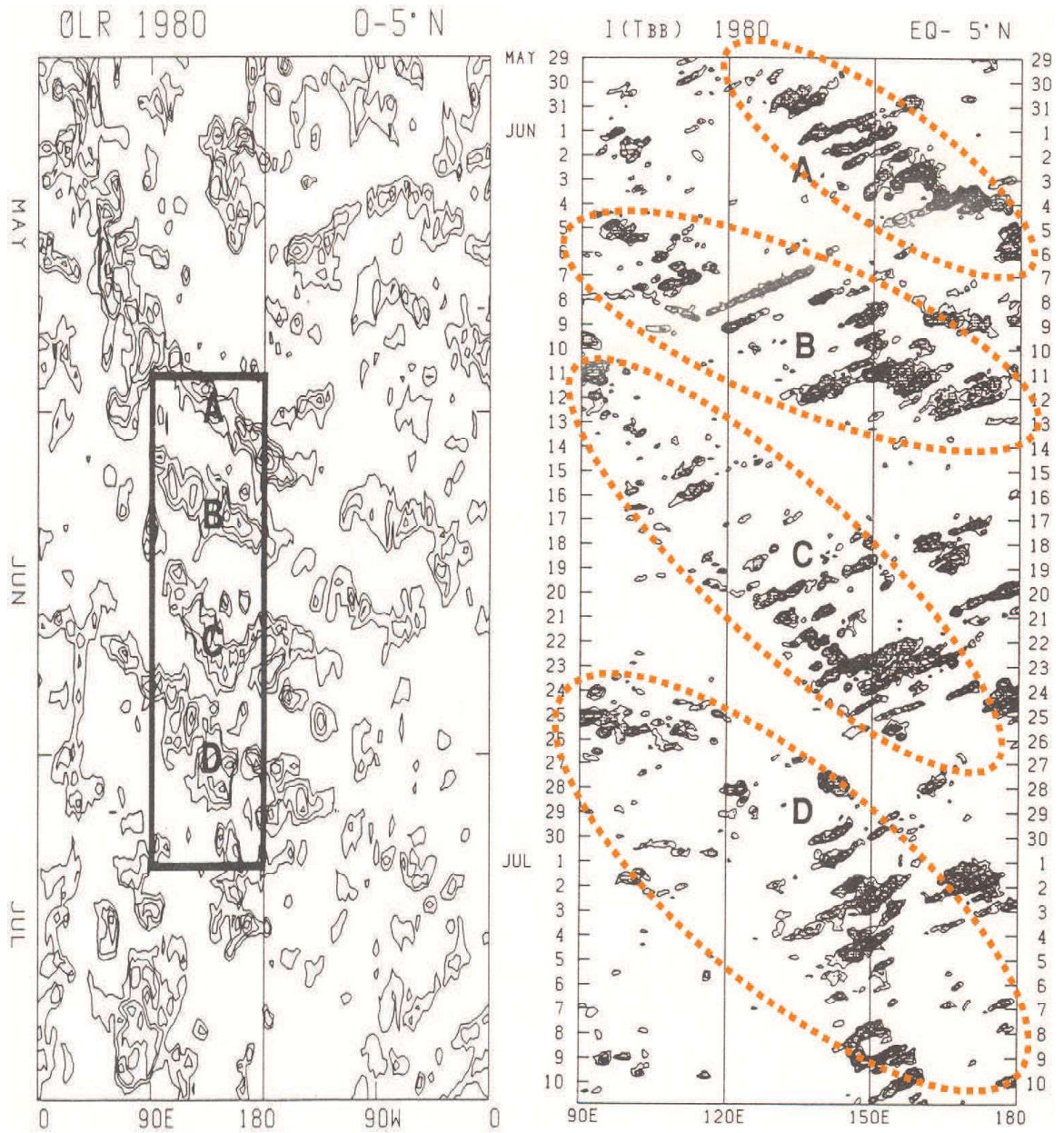


Figure 1.3: Reproduced from Nakazawa (1988). The figure on the left is a time-longitude section of transient (seasonal trend removed) OLR averaged between the equator and 5°N from May to July in 1980. Negative OLR anomalies are contoured in decrements of 30 W m^{-2} starting at -15 W m^{-2} . The letters **A**, **B**, **C**, and **D** label 4 super clusters. The figure on the right is a time-longitude section of the area mean black body temperature integrated between the equator and 5°N obtained from 3-hourly IR data from 29 May 00Z to 10 July 21Z, 1980 (corresponds to the thick-lined box in the left figure). The contour interval is 10 K and shading denotes regions where values are greater than 20 K. Dashed orange ellipses have been added to highlight the super clusters **A–D** composed of the westward propagating cloud clusters.

cause. Also noted was the observance of a Kelvin-like feature that appeared to be a distinct mode of synoptic-scale variability along the equator, though not unique to the convective envelope. The characteristics of this mode were reminiscent of Nakazawa's "super clusters" and were assumed to not play a major role in the evolution of the MJO.

A statistical study using radiosonde, reanalysis, and OLR data by Kiladis et al. (2005) examines the zonal and vertical structures of the MJO and their changes during eastward propagation. Fig. 1.4 displays a large-scale horizontal view of the MJO convection and circulation at 850 hPa and 200 hPa visualized through anomalous OLR (shading), streamfunction (contours), and winds (vectors). Some features to note at the 850 hPa level are the cyclonic Rossby gyres flanking the convection, the strong equatorial westerlies found to the west of and extending through the convection, and the broad, zonally long region of easterlies to the east of the convection. These circulation patterns have led to the general interpretation of the MJO flow as a convectively forced Rossby-Kelvin response. The heavy orange lines have been added to illustrate the zonal scale of the OLR minimum (darkest shading). Approximately 2/3 of this core convective region is contained within 20° of longitude. Noting that at the equator $111\text{ km} \approx 1^{\circ}$ of longitude, the east-west length of the entire minimum is $O(2000\text{ km} - 3000\text{ km})$. This scale is consistent with those found in other studies which have constructed composite MJO's using OLR data (Hendon and Salby, 1994; Hendon and Liebmann, 1994). Also consistent among these studies is the elliptical shape where the semi-major axis runs east-west. At the 200 hPa level there is divergent flow over and near much of the anomalous OLR region. Features corresponding to those in the low-level for a baroclinic structure can be seen (i.e., Rossby anticyclones, equatorial zonal winds of opposite sign from those at 850 hPa). This change in sign of the zonal winds with height is clearly seen in Fig. 1.5, which depicts the vertical structure of the zonal wind associated with Fig. 1.4. It is also evident that the magnitude of the upper-level zonal winds are approximately twice that of those in the low-level. The low-level westerlies are noticeably stronger than the low-level easterlies, though the easterlies have a longer zonal

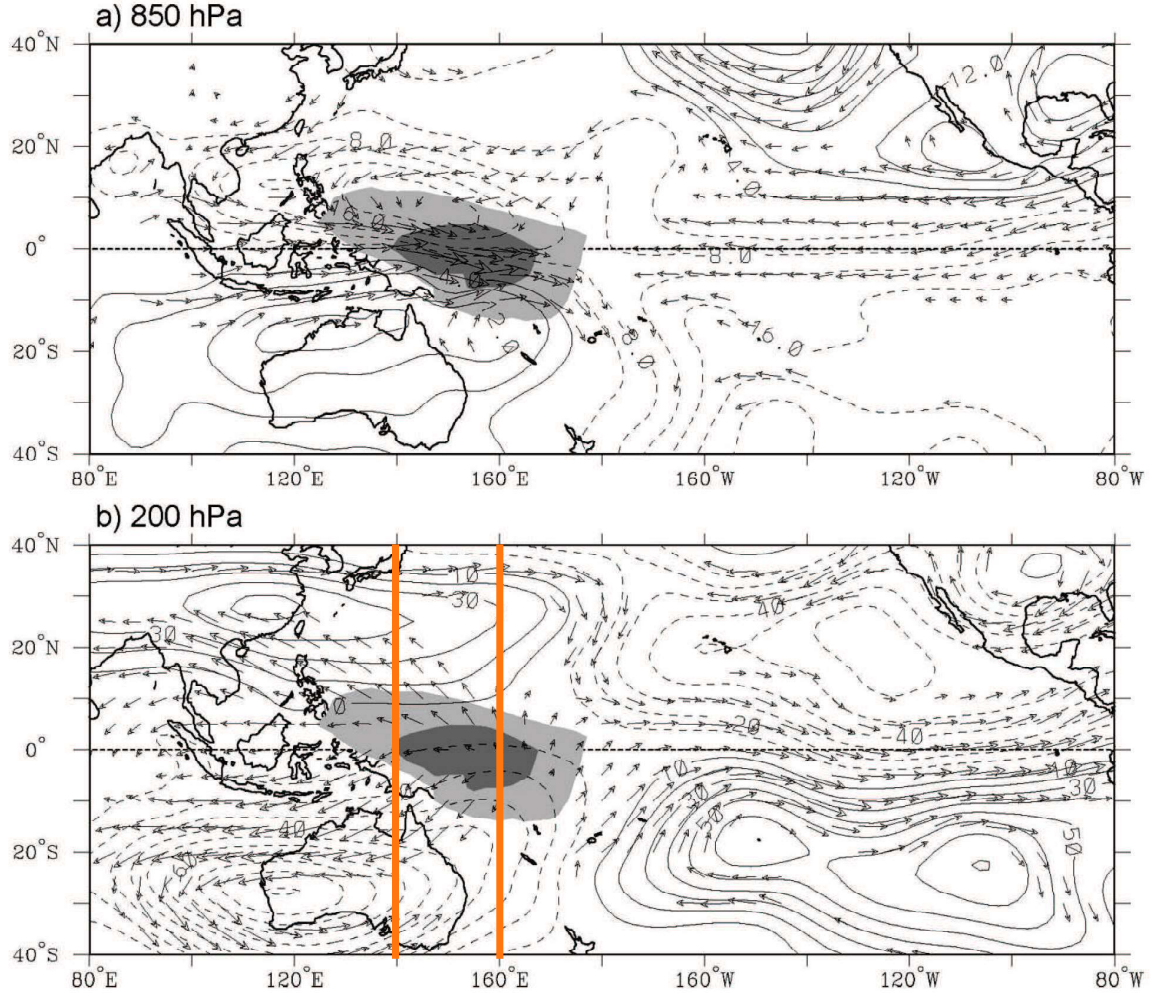


Figure 1.4: Reproduced from Kiladis et al. (2005). Anomalous OLR and circulation from ERA-15 reanalysis on day 0 associated with a -40 W m^{-2} perturbation in MJO-filtered OLR at the equator, 155°E for the period 1979–93, all seasons included; (a) 850 hPa and (b) 200 hPa. Dark (light) shading denotes OLR anomalies less than -32 W m^{-2} (-16 W m^{-2}). Streamfunction contour interval is (a) $4 \times 10^5 \text{ m}^2 \text{s}^{-1}$ and (a) $10 \times 10^5 \text{ m}^2 \text{s}^{-1}$. Locally statistically significant wind vectors at the 95% level are shown. The largest vectors are about 2 m s^{-1} in (a) and around 5 m s^{-1} in (b). The heavy orange lines in (b) have been added to delimit 20° of longitude over the OLR minimum.

extent. Notice that the OLR minimum is located within the low-level westerlies. This is stated to generally be the case, though the convective center can be found closer to the boundary between the low-level easterlies and westerlies. This structure is most likely to occur early in the lifecycle when the convection is over the Indian ocean, as the convection moves eastward, the low-level westerlies tend to push through and out in front of it.

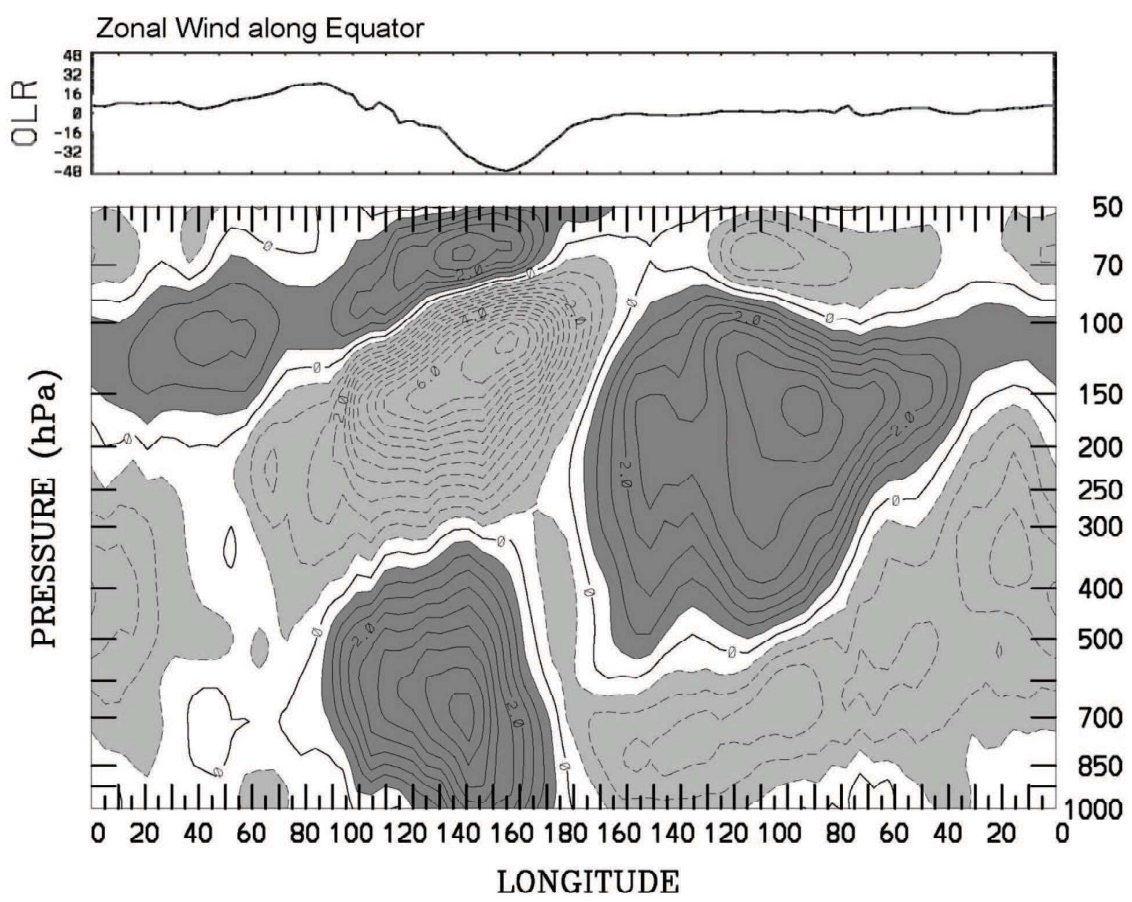


Figure 1.5: Reproduced from Kiladis et al. (2005). Zonal/height cross-section of anomalous zonal winds along the equator associated with Fig. 1.4. Contour interval is 0.5 m s^{-1} ; negative contours dashed. Dark (light) shading denotes anomalies greater than (less than) $\pm 0.5 \text{ m s}^{-1}$. The associated OLR anomaly along the equator is shown at the top in W m^{-2} .

The seasonality of the MJO in terms of low-level zonal winds and precipitation is documented by Zhang and Dong (2004). The main features can be summarized as follows: Near the equator, the MJO has a single peak season in the Indian and western Pacific oceans during the northern hemisphere winter. In the broader equatorial belt of the tropical Indian and western Pacific oceans the MJO migrates in latitude seasonally (see Fig. 1.6), and experiences two peak seasons. The primary peak season occurs during the northern hemisphere winter when the strongest signals are found between $5^\circ\text{--}10^\circ\text{S}$. The secondary peak season occurs in the northern hemisphere summer when the strongest signals are found between $5^\circ\text{--}10^\circ\text{N}$. This cross-equatorial migration is more pronounced in the western

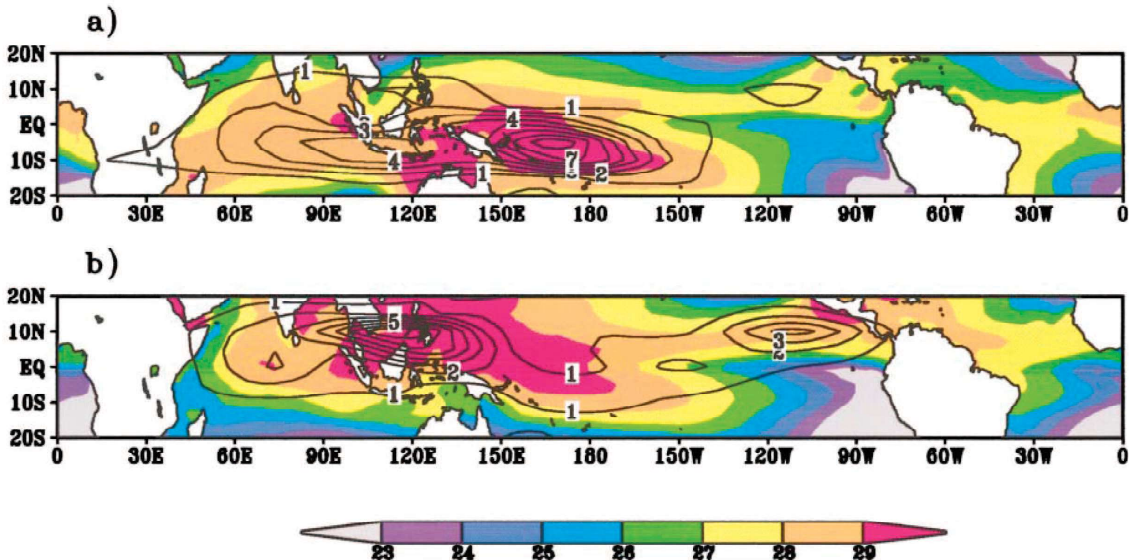


Figure 1.6: Reproduced from Zhang and Dong (2004). Zonal wind variance ($\text{m}^2 \text{s}^{-2}$, contours) at 850 hPa and mean SST ($^{\circ}\text{C}$, colors) averaged over (a) Dec–Mar and (b) Jun–Sep. Note the maximum zonal wind variance and SST during the northern hemisphere winter are in phase between 5° – 10°S , and are in phase between 5° – 10°N during the northern hemisphere summer. The stronger zonal wind variance signal during the northern hemisphere winter is also seen.

Pacific ocean than in the Indian ocean. Though it is tempting, Zhang and Dong warn against interpreting this seasonal migration as simply due to the seasonality of the sea surface temperatures (SST). One reason to believe it is more complex is that even though the MJO migration is in phase with the SST, their amplitudes do not match.

While complex models have some degree of success producing intraseasonal oscillations, understanding why can be difficult. Stripping away some of the complicated details by opting for a simplified theoretical model has helped in elucidating some of the basic dynamical concepts. The observed Rossby-Kelvin flow response associated with an MJO convective region hints at the usefulness of linear equatorial wave theory (Matsuno, 1966), which has formed the basis for investigating many tropical convection related phenomena (the MJO included). The “long-wave approximation” to the shallow water equatorial β -plane equations has been successful in producing analytical solutions for steady-state (Gill, 1980) and time-dependent (Heckley and Gill, 1984) localized diabatic forcing. Chao (1987)

considered the MJO using the “long-wave approximation” to the equatorial β -plane equations with a first internal baroclinic mode vertical structure, forced by a zonally propagating diabatic source. In solving the equatorial β -plane equations without introducing the “long-wave approximation” (Schubert and Masarik, 2006), chapter 2 of this research can be seen as the primitive equation generalization to Chao’s study.

Though not as manageable as linear systems, non-linear models can capture some of the richer detail which simpler frameworks are not capable of. This point is seen in research by Harris (1999), who uses a non-linear global shallow water model to study the effect of tropical convection on the large-scale atmosphere. Of particular interest to this research is a result regarding the dependence of Kelvin wave strength on the time-scale of forcing. By running simulations with different forcing time scales, the Kelvin and Rossby wave responses were seen to get stronger as the forcing time-scale became shorter. This was true down to a limit of approximately 2-3 days, at which point the response became dominated by gravity waves. When the forcing exists on this time scale, and is of large magnitude (“explosive” large-scale tropical convection), the Kelvin response is maximized and could influence the surrounding atmosphere as to trigger an MJO event. More specifically, if convection in the Indian Ocean became intense but short-lived, a strong Kelvin response could result, which could then couple with the convection and propagate eastward. Assuming this disturbance maintained a strong convective core which supported a Rossby response as well, this could be a potential mechanism (convectively-coupled Kelvin wave induced) for initiation of an MJO event.

Continuing upward in model sophistication, GCMs (general circulation model) are near the top due to their global scale, increasingly finer resolutions, and length of simulations. The state of GCM skill in producing intraseasonal oscillations is documented by Slingo et al. (1996), who reported the results from a subproject of AMIP (Atmospheric Model Intercomparison Project) focusing on the ability of 15 AGCMs (atmospheric general circulation model) to simulate the MJO. This was achieved by comparison of velocity po-

tential (χ) time-longitude data from the 15 models, with χ data compiled from European Centre for Medium-range Weather Forecasts (ECMWF) analysis (not reproduced here). Time-longitude diagrams of χ from the 15 models (2 realizations of the ECMWF model) are displayed in Fig. 1.7, in which the characteristics discussed below can be seen. The findings of this study can be summarized as follows: The models involved exhibited a wide range of skill in simulating the MJO. In terms of propagation direction alone, most models produced an eastward propagating χ anomaly, though some tended toward a standing oscillation, and at least one gave a chaotic field with no preference of propagation direction. Of the models that did produce a definite eastward propagating signal, the associated periodicities were reasonable though they tended to be shorter (25–30 days) than the analysis (40–50 days). Most models underestimated the strength of the signal, with the exception of GLA, NCAR, RPN, and UKMO. Most of the models were unable to capture the seasonality (Zhang and Dong, 2004) inherent to the MJO, with the exception of GLA, RPN, UKMO. None of the models produced a distinctive change in phase speed near the dateline as did the analysis (from 6 ms^{-1} to 16 ms^{-1} , due to the effect of convective decoupling from the Kelvin wave response). The conclusion is that among the models surveyed, a wide range of skill existed from complete inability, to reasonable resolution of several key features. Thus, while some models do exhibit a level of skill in simulating portions of an MJO, all contained significant deficiencies that need to be resolved before being able to claim simulation of an MJO “event”.

Analogous to GCM’s, theoretical work involving the MJO has had some degree of success, but still has deficiencies. To date, no theory has been given that adequately (completely) describes the MJO. It is likely though that some existing theory, or combinations thereof, explain aspects of the MJO. Many of the theories can be grouped under one of three types: (1) wave-CISK (Conditional Instability of the Second Kind) is based on the idea that the interaction between the Kelvin wave and the convection it is coupled to determine the eastward propagation of the MJO (Lau and Peng, 1987).

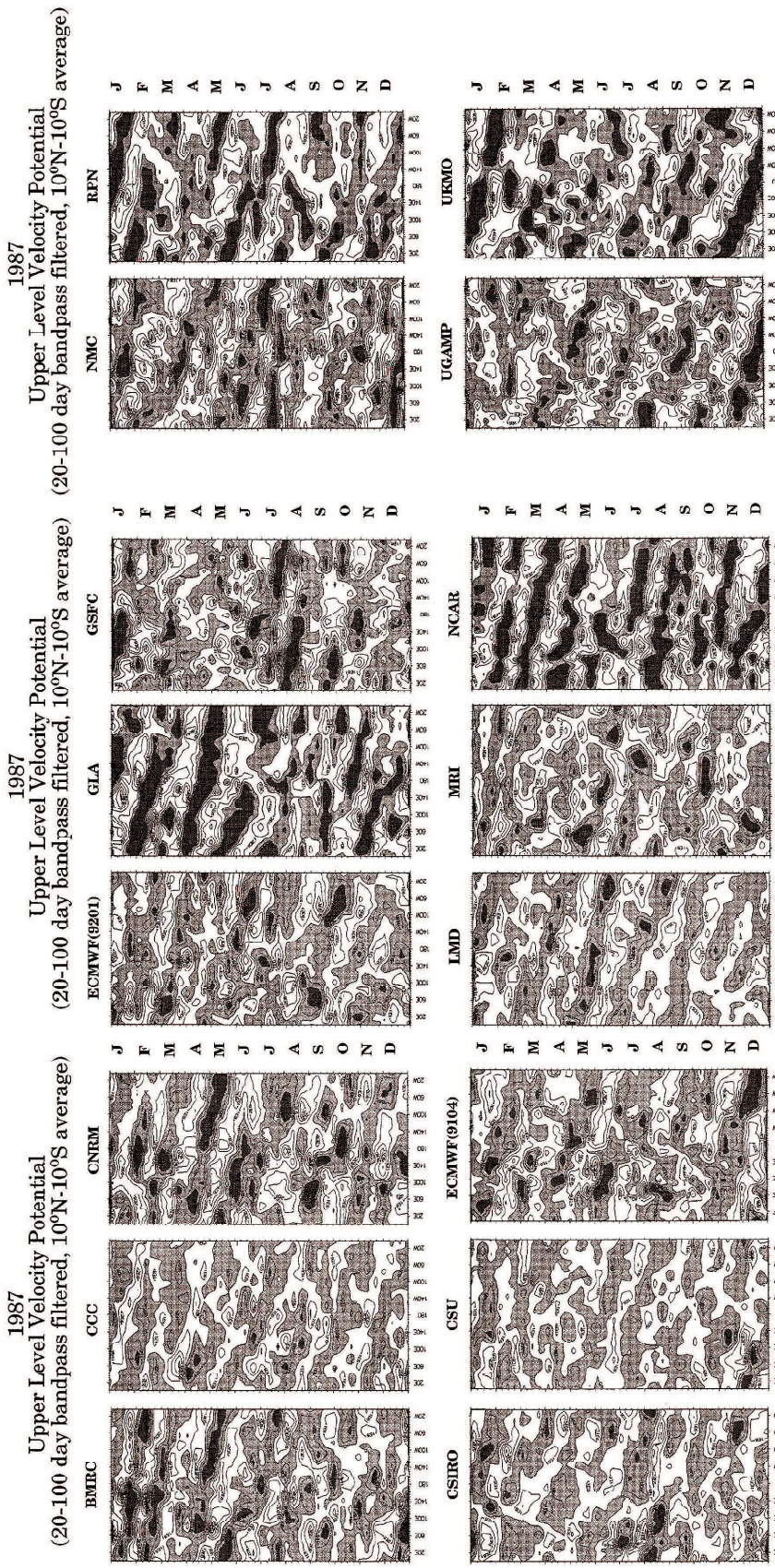


Figure 1.7: Reproduced from Slingo et al. (1996). Time-longitude diagrams for 1987 of the 20–100 day filtered velocity potential (χ) at 200 hPa (300 hPa for CCC), averaged between 10°N and 10°S, from the participating models. The model (institute) acronym is displayed above each diagram. Time increases downward. The contour interval is $1 \times 10^6 \text{ m}^2 \text{s}^{-1}$ for all models except GLA, NCAR, RPN, and UKMO where it is $2 \times 10^6 \text{ m}^2 \text{s}^{-1}$. Negative values are shaded.

The main problem with this theory is reconciling the observed phase speed with the required vertical scale. (2) WISHE (Wind-Induced Surface Heat Exchange) theory states that the waves which compose the MJO result from instability which is derived from the latent heat flux produced from wind-induced evaporation (Emanuel, 1987). A key problem with this is the assumption that the mean surface winds are easterlies, though the observed mean winds in the equatorial Indian and western Pacific oceans are westerlies. (3) Discharge-Recharge (Hu and Randall, 1994) proposes that non-linear interactions between radiation, cumulus convection, and surface moisture flux allow a stationary forcing which can periodically trigger MJO events. The time scale of the oscillation is thus determined by the time involved with drying of the atmosphere as an MJO event passes (“discharge”), and then the time required for the above mechanisms to remoisten the atmosphere so that it is primed for the next event (“recharge”). More detail on each of these theories can be found in Wang (2005).

As mentioned, it was only possible to cover a small portion of the extensive literature related to the MJO. The following reviews are suggested to learn more about the aspects introduced, and those which were not able to be included. An overview of the first 20 years of observational studies is presented by Madden and Julian (1994). A more recent paper, Zhang (2005), gives a concise survey of MJO topics including theoretical and modeling approaches. For a detailed treatment of intraseasonal variability (ISV) see Lau and Waliser (2005), in which each chapter is devoted to a particular aspect and the relevant literature has been reviewed by an authority in that area.

Lastly, two new papers utilizing up-to-date technology and data are listed. Preliminary results from an icosahedral-grid cloud-resolving AGCM (atmospheric general circulation model) are reported in Tomita et al. (2005), where simulations using 7 km and 3.5 km grid intervals produce an intraseasonal oscillation similar to the MJO. An analysis of the MJO using rainfall data from the TRMM satellite (Tropical Rainfall Measuring Mission) is presented in Benedict and Randall (2007).

1.3 Overview

Since its discovery 35 years ago much has been learned about the MJO, though in spite of the ample literature it has inspired, a satisfactory theory explaining it is elusive. This may not be surprising considering the complexities involved with a phenomenon that exists on an intraseasonal time scale, and across all spatial scales. With this in mind, a good approach may be to attack one piece of the puzzle rather than trying to solve the whole problem at once. We proceed by looking at an aspect of the MJO that has not been sufficiently explored—the extent to which the flow in the wake of the convective envelope can be interpreted as balanced and derivable from the potential vorticity (PV) field (Schubert and Masarik, 2006).

The motivation for this approach is as follows. Balanced theories, such as quasi-geostrophic theory and semi-geostrophic theory, provide a foundation for understanding the dynamics of midlatitude weather systems. These theories are more tractable than the primitive equations and can be succinctly expressed as two equations—a prognostic equation for the material conservation of potential vorticity, and a diagnostic equation (or invertibility principle) relating the potential vorticity to the streamfunction. In many tropical weather systems, such as the ITCZ and tropical cyclones, the release of latent heat plays a crucial role, so that potential vorticity is not materially conserved. However, even in these cases, a useful strategy is to formulate a balanced model that predicts the potential vorticity and then inverts it to find the associated balanced wind and mass fields. This approach has yielded insights into the dynamics of ITCZ breakdown and the formation of easterly waves (e.g., Schubert et al., 1991) and into the extreme PV structures that evolve in tropical cyclones (e.g., Hausman et al., 2006). What about large-scale weather systems that occur on the equator, such as the MJO? Are the concepts of balance and invertibility useful in understanding the essential dynamics of the MJO? Here we attempt to answer this question in the simplest context, i.e., in the context of a linearized equatorial β -plane model.

In the next chapter this simple theoretical model is used to explore the flow field

surrounding an eastward propagating forcing that is prescribed to coarsely resemble an MJO convective core. Analytical solutions are found and decomposed into equatorial wave components.

In chapter 3, the potential vorticity associated with the primitive equation model is calculated and a PV principle is derived. By considering an idealized version of the PV principle, a ratio which determines the magnitude of the PV anomaly is discovered. An invertibility principle is proposed based on an equatorial balance relation which allows us to invert the primitive equation PV.

Chapter 4 looks at the energy associated with the primitive equation solutions. We first derive a total energy principle, and then an associated Parseval relation. The Parseval relation allows computation of the total energy via spectral sums which has the advantage of being easier to calculate than a physical space integral, as well as the ability to partition the energy among the equatorial wave types. Lastly, the dependence of the response energy on the forcing parameters is studied using the Parseval relation.